Beryllium doping of GaAs and GaAsN studied from first principles

Hannu-Pekka Komsa,[1,*] Eero Arola,[1] Janne Pakarinen,[2] Chang Si Peng,[2] and Tapio T. Rantala[1,†]
[1]*Department of Physics, Semiconductor Physics Laboratory, Tampere University of Technology, FIN-33101 Tampere, Finland*
[2]*Optoelectronic Research Centre, Tampere University of Technology, FIN-33101 Tampere, Finland*
(Received 29 September 2008; revised manuscript received 13 February 2009; published 20 March 2009)

We have studied beryllium defects in GaAs and GaAsN from first principles, concentrating on the nitrogen effect on the defect formation and the beryllium effect on the nitrogen alloying properties. Due to the small size of both species the defect complexes and clusters take an important role. In particular, we consider the role of the (Be-N) split interstitials and the beryllium interstitials near substitutional beryllium. These are found to be responsible for the charge-carrier compensation in Be-doped GaAsN. Also, any nitrogen tied to the (Be-N) defects is unable to contribute to the conventional GaAsN alloy properties. We also briefly comment on the implications to the beryllium diffusion.

DOI: 10.1103/PhysRevB.79.115208 PACS number(s): 71.55.Eq

I. INTRODUCTION

Beryllium is one of the most widely used *p*-type dopants in GaAs and also other III-V semiconductors. Lately, studies on growth of beryllium doped (In)GaAsN revealed some interesting phenomena: (a) introducing nitrogen into the growth of Be-doped GaAs compensates the *p*-type carrier concentration[1–3] and (b) introducing beryllium into the growth of GaAsN increases the nitrogen concentration of the sample.[1,4] Subsequent annealing seems to have only a minor effect on the carrier concentration of solid-source molecular-beam epitaxy (SSMBE) grown samples.[1]

Moreover, beryllium is known to diffuse strongly in GaAs and it also has a strong effect on the interdiffusion of In and Ga within the InGaAsN-based quantum wells (QW).[5] This in turn has an effect on the electrical and optical quality of the material. It is found, e.g., that beryllium decreases the In diffusion of InGaAs QWs. Recently, there have been a few studies on the diffusion of the beryllium in (In)GaAs,[6,7] but unfortunately many of the parameters simply need to be guessed in the lack of better estimates. The effect of Be doping on the Be diffusion and on the interdiffusion in pure GaAsN seems to be still largely unknown.

Both doping and diffusion properties are closely tied to the energetics of the defects. For some reason, the first-principles studies of beryllium defects even in GaAs, let alone GaAsN, are missing. Beryllium passivation by hydrogen in GaAs was studied in Ref. 8 and Be doping of GaN was studied in Refs. 9 and 10. Explicit diffusion calculations from first principles are presently mostly restricted to the evaluation of energy differences between configurations or the energy barrier height involved in the typical diffusion processes. This still enables us to find out the likely charge states of the defects involved in the diffusion processes. In addition, doping of GaAsN presents a more fundamental area of study: how do the defect energetics and electronic structure change in the vicinity of nitrogen, which is an isovalent impurity with much smaller size and higher electronegativity than arsenic. It is known that nitrogen has a strong effect on the nearest-neighbor site (gallium) atoms, and as beryllium likes to occupy gallium site, significant structural, electronic, and optical effects can be expected. There is significant strain around nitrogen and beryllium, and the relief of this strain can make some complexes energetically favored. Furthermore, the small beryllium atom can easily fit into different locations in the crystal, exhibiting both donor and acceptor behaviors on the interstitial and substitutional sites, respectively. This makes the study quite challenging, especially in the case of GaAsN.

Other defects in GaAsN have been studied to some extent. Yu *et al.*[11] found that doping with Si leads into mutual passivation of both the electrical activity of Si and the band-gap reduction due to nitrogen. This was originally explained to result from the Si_{Ga}-N_{As} defect, but later on suggested to be due to the $(Si\text{-}N)_{As}$ split interstitial.[12] Li *et al.*[13] examined several donors in Ga and As sites near to N_{As}. Moreover, hydrogenation of GaAsN has been studied rather extensively. Similar nitrogen deactivation has been found[14] and employed to fine tune the nitrogen concentration. Several computational groups have tackled the issue thereafter.[15–18]

II. COMPUTATIONAL METHOD

We use the "standard" formalism to determine the prevalent types and transition levels of the defects.[19] The formation energy is defined as

$$E^f[X^q] = E_{\mathrm{tot}}[X^q] - E_{\mathrm{tot}}[\mathrm{bulk}] - \sum_i n_i\mu_i + q[E_F + E_v + \Delta V], \tag{1}$$

where $E_{\mathrm{tot}}[X^q]$ is the total energy of the supercell with the defect X (in the charge state q) and $E_{\mathrm{tot}}[\mathrm{bulk}]$ is the total energy of the supercell of bare GaAs or GaAsN bulk, depending on the case. The chemical potentials μ_i of n_i added or removed atoms allow us to describe various growth conditions. E_v is the valence-band maximum (VBM) at Γ point in the bulk material, E_F is the Fermi energy with respect to E_v, and ΔV is the shift term used to align the potentials in between the two supercells.

There is still ongoing debate on the validity of this type of defect calculations where especially the finite-size effects are known to be important.[20] However, for a large number of configurations presented here, the finite-size scaling method

becomes computationally laborious. Even if this was done, the band-gap problem is still present.[21] Instead, we will calculate with just one supercell and try to carefully cope with the limitations. We will also employ the potential alignment correction [ΔV term in Eq. (1)] as it has been shown to give rather good results, even if theoretically not well motivated.[22]

For the shallow defects (only Be_{Ga} in this paper), the periodic-image interaction (defect potential overlap) is very strong, and consequently the defect states in the periodic lattice do not form a flat band, but more of a slightly perturbed host band. In this case, taking the VBM energy as the average of the highest valence band over the Brillouin zone (BZ), which is at about 120 meV below the Γ-point value, appears to give better results, although somewhat *ad hoc*. Moreover, shallow defect levels tend to follow band edges, while deep defect levels do not.[21] Due to these uncertainties, we show both band-gap limits in our formation energy diagrams and the interpretation should be done carefully and estimating the shallowness or locality of the defect states.

With the defect formation energies at hand, the defect concentrations can be calculated as

$$c = N_{\text{sites}} N_{\text{config}} \exp(-E^f/kT), \tag{2}$$

where the number of equivalent sites is about 2.2×10^{22} cm^{-3} and only one configuration, for both the substitutional and the interstitial defects. When applying this equation we choose 450 and 800 °C to simulate typical GaAsN growth and annealing temperatures, respectively.

All calculations, within the density-functional theory (DFT) framework and employing local-density approximation (LDA) with projector-augmented waves (PAW), were done using VASP (Vienna *ab initio* simulation package).[23–25] In case of gallium the 3*d* electrons are treated as valence electrons. For the defect calculations we use 216-atom supercells with $2\times2\times2$ Monkhorst-Pack **k**-point mesh and 400 eV cutoff energy. For the density of states (DOS) we use $5\times5\times5$ **k**-point mesh. Atomic relaxation for all configurations and charge states is performed until forces are less than 10 meV/Å. For defect calculations in GaAs we use the calculated lattice constant of pure GaAs (5.605 Å), and similarly for defects in GaAsN we use the calculated lattice constant of GaAsN (5.596 Å). 216-atom supercell limits the minimum beryllium concentration to about 0.9% or 2×10^{20} cm^{-3}. However, the actual concentration in the low-concentration limit plays hardly any role in the electronic and atomic structure if the supercell finite-size effects are vanishingly small. For most deep defects, 216-atom supercell should be large enough. Similarly, the minimum nitrogen concentration is about 0.9%, which is rather realistic from the experimental viewpoint.

Regarding the chemical potentials, in the arsenic-rich limit the arsenic atom chemical potential is that of a bulk arsenic atom, and gallium chemical potential comes from the equilibrium condition with GaAs: $\mu_{\text{Ga}} = \mu_{\text{GaAs}} - \mu_{\text{As}}$. The gallium-rich limit follows similarly. For the beryllium chemical potential in GaAs we have chosen that of beryllium bulk. This choice gives a rather high chemical potential and consequently low formation energies. Still, in the lack of a better choice, we settle for this, and the results are easy to adjust later if needed. For the Be in GaAsN case, there is a better choice, namely, a Be_3N_2 compound, in which case we get

$$3\mu_{\text{Be}} + 2\mu_{\text{N}} = 3\mu_{\text{Be[bulk]}} + 2\mu_{\text{N[N2]}} + \Delta H_f[\text{Be}_3\text{N}_2]. \tag{3}$$

The experimental heat of formation ΔH_f is −6.11 eV per f.u.[26] This could be used to obtain a better estimate for μ_{Be}, but then a value for μ_{N} is required. However, in our calculations, we do not need the nitrogen chemical potential as all the calculations have an equal number (one) of nitrogens in a supercell (also in the case of the GaAsN bulk), and therefore in the results it is sufficient to use μ_{Be} taken from the Be bulk. This also makes the comparison easier, and we do not have to worry about the practical problems: validity of Eq. (3) is questionable in the growth of dilute GaAsN, and the situation on the surface is very different from the bulk and should be considered separately.

III. RESULTS AND DISCUSSION

The formation energies of all defects are collected in Table I. We give the numeric results in the case of arsenic-rich growth conditions. In the formation energy diagrams in Fig. 1, both the gallium and arsenic-rich cases are shown.

This section is divided into three parts: first, computational results of beryllium defects in GaAs are covered briefly. Second, beryllium defects in GaAsN are covered in contrast to the respective GaAs cases. Finally, our computational results are compared to the recent experimental results.

A. Beryllium in GaAs

Since Be doping of GaAs results in a strong *p*-type carrier concentration of almost the same as the total beryllium concentration, it would seem that most of the beryllium is in the gallium-substitutional site. Rest of the beryllium can be expected to be in the interstitial sites. In addition to a gallium-substitutional beryllium Be_{Ga}, we also study interstitial beryllium on the two inequivalent sites of the zinc-blende lattice: in the middle of the arsenic (tAs) and gallium (tGa) tetrahedra.[27] Moreover, since interstitial atoms like open spaces and such a space is opened whenever beryllium substitutes gallium, inserting another beryllium atom on an interstitial site (gallium tetrahedron) near Be_{Ga} results in a beryllium cluster (Be_{Ga}-Be_I), which could be expected to have a rather low formation energy.

Formation energies of beryllium related defects in GaAs are shown in Fig. 1, and in Table I. The native defects, V_{Ga} and Ga_I, are extensively covered in the literature (e.g., all native defects in Ref. 28, self-interstitials in Ref. 29, and vacancies in Ref. 30) which therefore can be used to check the validity of our calculations or possibly to "calibrate" our results with the other studies.

There is indeed some variance in the results of the gallium vacancy in the literature. The literature results are shifted to the As-rich limit for the comparison where needed. Our results are in a very good agreement with the computational results of Janotti *et al.*[15] who find 2.9 eV for V_{Ga}^{-3} and ionization levels below 0.2 eV. Formation energies are also in

TABLE I. Formation energies at the arsenic-rich limit with Fermi-energy E_F=0 with respect to VBM. Also shown are the different bond lengths of the defect atoms with the neighboring atoms. For reference, Ga-As bond length in GaAs is 2.427 Å. Energies are in the units of eV and distances in the units of Å.

	Energy (eV)			Bond lengths (Å)					
				GaAs		GaAsN (near)			
Configuration	GaAs	GaAsN (near)	GaAsN (far)	Be-Ga	Be-As	Be-Ga	Be-As	Be-N	Ga-N
V_{Ga}^{0}	2.465	2.351	2.461						1.890
V_{Ga}^{-1}	2.554	2.383							1.890
V_{Ga}^{-2}	2.698	2.459							1.890
V_{Ga}^{-3}	2.879	2.609	2.825						1.889
Be_{Ga}^{0}	−0.082	−0.215	−0.096		2.252		2.379	1.741	2.025
Be_{Ga}^{-1}	−0.150	−0.290	−0.178		2.253		2.377	1.744	2.025
Be_{As}^{+1}	3.403			2.250					
Be_{As}^{0}	3.527			2.198–2.267					
Be_{As}^{-1}	3.691			2.203					
Be_{As}^{-2}	3.989			2.141–2.198					
Be_{As}^{-3}	4.393			2.129					
$Be_{I(tAs)}^{+2}$	1.442	1.470	1.457	2.889	2.391	2.543/3.267	2.223	3.289	2.048/2.021
$Be_{I(tAs)}^{+1}$	2.185	2.095		2.882	2.389	2.589/3.072	2.245	3.097	2.033/2.021
$Be_{I(tAs)}^{0}$	3.013	2.755	2.994	2.877	2.388	2.671/2.794	2.317	2.965	1.976/2.023
$Be_{I(tGa)}^{+2}$	2.129	1.581		2.539/2.542	2.775/2.781				
$Be_{I(tGa)}^{+1}$	2.674			2.516/2.522	2.786/2.793				
$Be_{I(tGa)}^{0}$	3.418	1.399	3.428	2.489/2.494	2.796/2.806	2.058/3.475	2.206	3.903	1.847/2.036
$Ga_{I(tGa)}^{+3}$	2.745								
$Ga_{I(tGa)}^{+2}$	2.623								
$Ga_{I(tGa)}^{+1}$	2.485								
$Ga_{I(tGa)}^{0}$	3.407								
$Ga_{I(tGa)}^{-1}$	4.338								
$Ga_{I(tAs)}^{+1}$	2.737								
$Ga_{I(tAs)}^{0}$	3.697								
$(Be_{Ga}\text{-}Be_I)^{+1}$	0.943	0.140		2.764	2.141/2.312/2.359	2.966	2.182	1.600	2.040
$(Be_{Ga}\text{-}Be_I)^{0}$	1.688	0.711		2.675	2.149/2.349/2.352	2.802	2.169	1.534	2.028
$(Be_{Ga}\text{-}Be_I)^{-1}$	2.640	1.097		2.630	2.149/2.347/2.357	2.664	2.184	1.508	2.016
$(Be_{Ga}\text{-}Ga_I)^{0}$	2.065								
$(Be\text{-}N)_{As(100)}^{0}$		1.446				2.258/2.775		1.456	1.885/3.191
$(Be\text{-}N)_{As(100)}^{-1}$		2.087				2.194/2.726		1.481	1.855/3.186
$(Be\text{-}N)_{As(100)}^{-2}$		3.011				2.149/2.681		1.508	1.827/3.186
$(Be\text{-}N)_{As(111)}^{0}$		1.086				2.078/2.614		1.487	2.030
$(Be\text{-}N)_{Ga}^{+2}$		0.830					2.166/2.812	1.551	
$(Be\text{-}N)_{Ga}^{0}$		0.680					2.169/2.801	1.545	

agreement with Ref. 30: about 2.5 eV for V_{Ga}^{0} although their ionization levels are higher, possibly due to their larger computational band gap or the Makov-Payne corrections, and therefore also the V_{Ga}^{-3} formation energy is somewhat higher. Zhang and Northrup[28] found clearly higher formation energy of about 4 eV for V_{Ga}^{0}. Experimental values from Gebauer *et al.*[31] are also higher at 3.2 ± 0.5 eV for V_{Ga}^{0}. The experiments should be somewhat arsenic rich, although direct comparison is of course difficult. Moreover, only the sum of the ionization level energies can be extracted from the experiments, which seems to agree with higher levels.

Our results for the interstitial gallium Ga_I follow very closely those of Ref. 29. The defect prefers +1 charge state for most of the Fermi energies. The site within a gallium tetrahedron is slightly preferred over the arsenic tetrahedron for all charge states: 290 meV for neutral and 250 meV for +1 charge states, compared to 310 and 270 meV in Ref. 29, respectively.

Beryllium on a gallium site is a shallow acceptor with the measured ionization energy of about 28 meV.[32] Using the

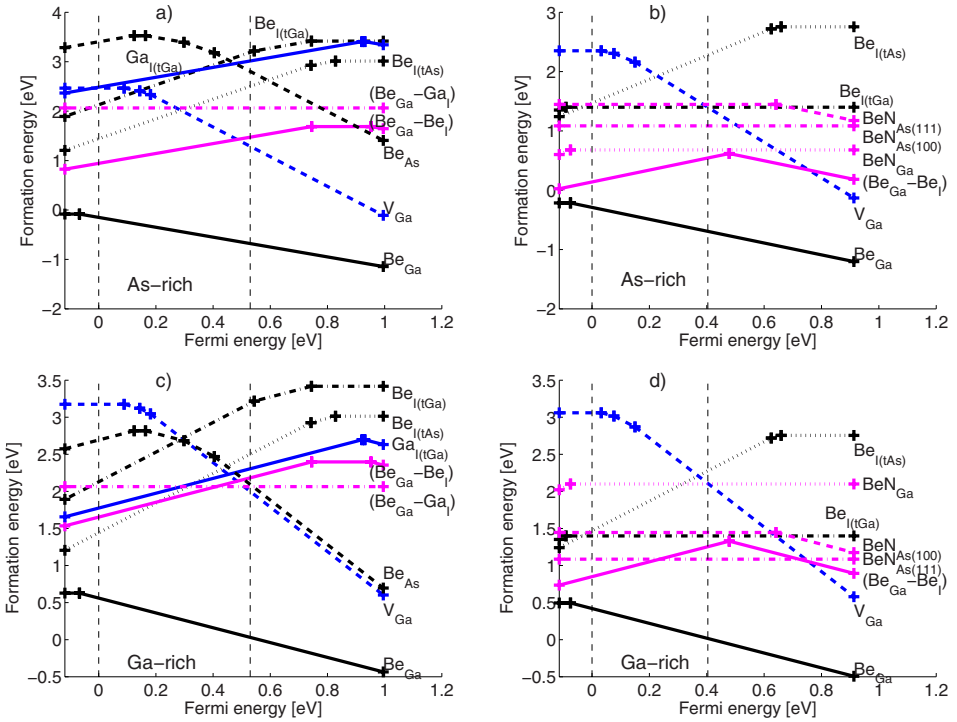

FIG. 1. (Color online) Formation energy diagram of native and beryllium related defects in [(a) and (c)] GaAs without nitrogen on the left and [(b) and (d)] in GaAsN on the right. [(a) and (b)] Arsenic-rich cases are shown on the top and [(c) and (d)] gallium-rich cases on the bottom. Vertical dashed lines give the GaAs bulk VBM and CBM at the Γ point, while the *x* axis spans the Fermi-energies from the BZ-averaged VBM to the BZ-averaged CBM. Color coding: simple Be-related defects with black, GaAs native defects with blue, and defect complexes with magenta.

BZ-averaged VBM, we get the acceptor ionization energy of about 50 meV. One could suspect that the Be_{Ga} formation energy is incorrect due to the strong defect-defect interaction between the supercells. However, our calculation on a smaller 64-atom supercell gives very similar results. Be-As bond length has shortened to 2.25 Å from that of the bulk Ga-As bond length 2.43 Å.

Due to the −3 charge state, beryllium on an arsenic site Be_{As} can have low formation energy only in a strongly *n*-type material (and gallium-rich growth), but this is an unlikely scenario for Be-doped GaAs(N). Interestingly, Be_{As} can behave both as an acceptor and as a donor. We find that with noninteger number of electrons in the supercell, the geometry is asymmetric: all four Be-Ga bond lengths are slightly different.

Interstitial beryllium likes to stay on the tAs site and predominantly on the +2 charge state. It has ionization levels slightly below conduction-band minimum (CBM) corresponding to Be-related states with *s* character. Judging also from the fact that Be-As or Be-Ga distances do not change at different charge states, $Be_{I(tAs)}$ appears a lot like free Be atom. $Be_{I(tGa)}$ would seem to have some bonding character with the surrounding gallium atoms.

The $(Be_{Ga}$-$Be_I)$ complex acts as an amphoteric defect, which at the neutral charge state can be quite well described by a Be_I^{+1} accepting one electron from a neighboring Be_{Ga}^{-1}. Indeed, in the local density of states (LDOS) we can find a high lying state with weight mostly on the interstitial beryllium, similar to Be_I. The substitutional beryllium displacement is only 0.28 Å and the interstitial beryllium 0.67 Å. Be-Be distance is 2.013, 2.035, and 2.043 Å for +1, 0, and −1 charge states, respectively. We also tested the possibility of (Be-Be) dimers on a gallium site, but all configurations relaxed to the same $(Be_{Ga}$-$Be_I)$ geometry. Further clustering of beryllium is also possible, but not investigated here.

All in all, in order to get the strong *p* doping that Be-doped GaAs exhibits, there should not be present high concentrations of any compensating (donorlike) defect species. This indeed seems to be the case, as seen in Fig. 1.

The chemical potential matching the experimental conditions is often indeterminate, and therefore, we will mostly refrain from giving out absolute defect concentrations. Note, however, that changing the beryllium chemical potential does not change the relative concentrations of the defects with the same number of beryllium atoms as can be deduced from Eqs. (1) and (2). The solid solubility limit of beryllium in GaAs, mostly consisting of Be_{Ga}, is rather well defined and well known: about 10^{20} cm^{-3} depending on the growth temperature, but not radically on the As/Ga pressure ratio.[33] In the As-rich limit, the Be_{Ga} concentration from the calculated formation energy, however, is unrealistically high (due to high μ_{Be}). The Ga-rich limit gives about 1×10^{18} and 3×10^{19} cm^{-3} for 450 and 800 °C, respectively. The growth (thermo)dynamics apparently limits the maximum obtainable total beryllium concentration.

In Ref. 33, it was also found that beryllium diffusion is much weaker in the case of the high As/Ga ratio. This could be well explained by looking at the Be_I/Be_{Ga} ratio obtained from our calculations at the As-rich and Ga-rich limits. The Be_I formation energy is independent of the μ_{Ga} (or μ_{As}) chemical potential and giving about 4×10^{15} cm^{-3} at 800 °C. This concentration should give us an upper limit for the beryllium interstitials in equilibrium and it is somewhat smaller than the values often assumed in the literature (see e.g., Table II in Ref. 6). However, the Be_I/Be_{Ga} ratio is about 3×10^{-6} and 3×10^{-11} at 450 °C in the Ga- and As-rich limits, respectively, and similarly 2×10^{-4} and 7×10^{-8} at 800 °C. The very small concentration of Be_I in As-rich environment naturally explains the weak diffusion. We note that, in the above estimate we ignored the $(Be_{Ga}$-$Be_I)$ com-

plex. For them, $N_{\text{sites}}N_{\text{config}}$ in Eq. (2) is about $4N_{\text{Be}_{\text{Ga}}}=4\times10^{20}$ cm^{-3}. Formation energies of 0.94 eV (As-limit) and 1.65 (Ga-limit) give then 2×10^{16} and 7×10^{12} cm^{-3}, respectively, at 800 °C. That is, in the As-rich limit, (Be_{Ga}-Be_{I}) induces a meaningful increase in interstitial Be concentration, but the total interstitial concentration should still be below 10^{17} cm^{-3} at 800 °C.

For this material, the important aspects concerning diffusion are the beryllium interstitial diffusion and the kick-out reactions.

From Table I, we can see that most of the Be_{I} is in the +2 charge state, while Ga_{I} has comparable energies in +1, +2, and +3 charge states. For the beryllium in the interstitial sites, the position inside the arsenic tetrahedron is favored in all the charge states. The energy difference between the formation energies of the tGa and tAs sites increases from 405 to 687 meV with increasing positive charge. Our reaction path tests using the nudged elastic band method show that the potential barrier is very small (in the order of tens of meV), and therefore just the energy difference between the end-point calculations should give quite a good estimate of the real barrier height. Regardless of the charge state, this value is quite small even for the highest concentration $\text{Be}_{\text{I}}^{+2}$ and shows why beryllium diffuses so well in GaAs.

First estimate for the kick-out energy can be obtained from the calculated formation energies. We have also calculated the energy related to the final configuration right after the kick out (i.e., the nearest site configuration). The (Be_{Ga}-Ga_{I}) configuration, where Ga_{I} resides next to Be_{Ga}, is always in the neutral charge state, whose formation energy is almost 1 eV below that of the interstitial neutral $\text{Be}_{\text{I(tAs)}}$. In a *p*-doped sample, we should compare to a charged Be_{I}, in which case $\text{Be}_{\text{I}}^{+2}$ has essentially lower energy than $(\text{Be}_{\text{Ga}}\text{-}\text{Ga}_{\text{I}})^{0}$, while the formation energy of $\text{Be}_{\text{I}}^{+1}$ is close to it. Decomposing the (Be_{Ga}-Ga_{I}) into isolated $\text{Be}_{\text{Ga}}^{-1}$ and $\text{Ga}_{\text{I}}^{+1}$ requires further about 270 meV. Finally, related to this, it is clear that mobile Be_{I} is also eager to fill all the gallium vacancies.

B. Beryllium in GaAsN

For the GaAsN study, we need to consider almost all of the defect configurations of GaAs and additionally a few (Be-N) complexes. To complicate things further, a new configurational degrees of freedom, namely, the number of nitrogen in the local atomic environment of the defect, emerges. Fortunately, nitrogen concentration is usually very small, so that it should be sufficient to investigate only the cases of the defect near nitrogen or further away from the nitrogen. In all of the calculations, there is only one nitrogen atom in the 216-atom supercell resulting in a 1% nitrogen concentration. This is advantageous in the case of the DFT-LDA calculations as the band gap is still relatively large.

The formation energies are shown in Fig. 1 and listed in Table I. First of all, we point out from the Table I, that the formation energies of the defects far from nitrogen are always close to those of pure GaAs. This has two important implications: (1) the effect of nitrogen on the defect formation out of the nearest-neighbor sites is quite minimal, and (2) if the ionization levels of deep defects far from nitrogen are not affected by the decrease in the band gap from GaAs to GaAsN (about 100 meV) they are probably also quite insensitive to the LDA band-gap error. Because of (1), from here on, we expect the beryllium energetics in GaAsN out of the nearest-neighbor site of the nitrogen to follow closely that of GaAs.

We find that the vacancy formation near nitrogen is preferred in all charge states, being 115 meV for V_{Ga}^{0} and 204 meV $\text{V}_{\text{Ga}}^{-3}$. This was already reported in Ref. 15, although their energy lowering was somewhat higher, 0.43 eV for $\text{V}_{\text{Ga}}^{-3}$. We would also like to explain this effect in a different way: when nitrogen atom is introduced substitutionally into GaAs, the Ga-N bond is stretched to 2.04 Å as compared to the 1.93 Å in GaN, but when one of the gallium atoms is removed, nitrogen is able to relax closer to the three remaining gallium atoms (displaced about 0.44 Å from the zinc-blende anion site) resulting in the Ga-N bond length of 1.89 Å. The bond length remains the same for all charge states meaning that there is no interaction with the vacancy.

Rather surprisingly, also Be_{Ga} is about 130 meV more likely to form near nitrogen than far away from it. This is not easy to explain with the geometric considerations similar to the gallium vacancy. Here, beryllium moves 0.19 Å from the already stretched Ga site (or 0.58 Å from the ideal lattice site) closer to nitrogen, which keeps close to the original position. The more likely cause is the strong Be-N bond and the effect of Be on to the Ga 3*d*-N 2*s* interaction. The former is supported by the short Be-N bond length, although the changes in the corresponding LDOS with respect to GaAsN in Fig. 2 are small. The latter is supported by the large beryllium weight increase at around −15 eV such that beryllium mixes with the Ga 3*d* and N 2*s* states. The beryllium weight matches well with the nitrogen weight at this energy range.

The neutral $\text{Be}_{\text{I(tAs)}}$ configuration might be expected to have clearly lower formation energy near the nitrogen and this is indeed the case: almost 260 meV difference is found. However, this does not hold for the positive charge states, and in the +2 charge state $\text{Be}_{\text{I(tAs)}}$ is slightly more likely to form far from nitrogen. Both the nitrogen and beryllium are pushed farther from each other from their ideal positions. At the positive charge state nitrogen returns close to its original position, but beryllium is even more strongly displaced from the tAs site to a location between the tAs and tGa sites. This could be explained with the steric effects: when nitrogen pulls gallium atoms closer to itself, the gallium atoms also push beryllium farther from nitrogen. The repulsion is intensified in the positive charge states since gallium atoms have positive ionic nature. The high electronegativity of nitrogen atom also increases the positive charge character of the nearest-neighbor gallium atoms.

Introduction of nitrogen also breaks the symmetry in such a way that there are now two inequivalent positions for the $\text{Be}_{\text{I(tGa)}}$ near nitrogen (and with the same distance to nitrogen): beside the tAs interstitial site at $(\frac{3}{4},\frac{3}{4},\frac{3}{4})$ and beside a gallium atom at $(-\frac{1}{4},-\frac{1}{4},-\frac{1}{4})$.[27] Already in the GaAs lattice, $\text{Be}_{\text{I(tGa)}}$ has only a very small barrier with respect to relaxation to the $\text{Be}_{\text{I(tAs)}}$ site, and in the nitrogen neighborhood the barrier disappears for the former location. $\text{Be}_{\text{I(tGa)}}$ at the latter

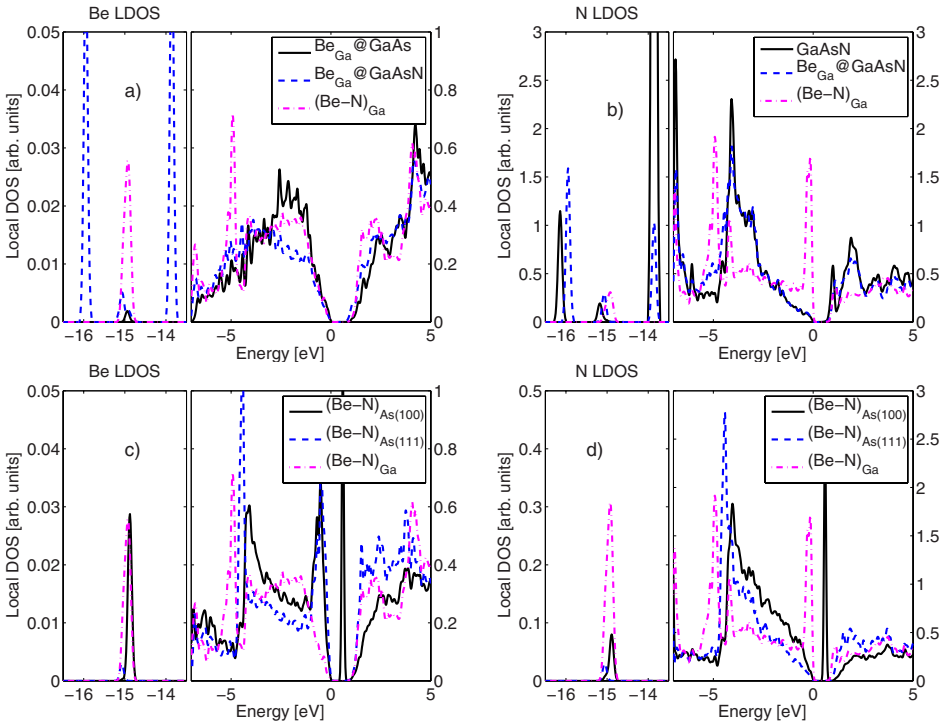

FIG. 2. (Color online) The local density of states of [(a) and (c)] Be and [(b) and (d)] N related electronic states for selected configurations displaying the [(a) and (b)] changes in the alloying properties and [(c) and (d)] comparison of the split-interstitial defects. The energy zero is set at the valence-band maximum.

location is interesting because beryllium moves close to a gallium site, gallium moves halfway between Be and N, and N also moves considerably out of the ideal site, therefore creating a kind of three-atom split-interstitial $(\text{Be-Ga})_{\text{Ga}}+(\text{Ga-N})_{\text{As}}$ or $(\text{Be-Ga-N})_{(\text{GaAs})}$. $\text{Be}_{\text{I(tGa)}}$ in Table I is the latter configuration.

In GaAsN, the $(\text{Be}_{\text{Ga}}\text{-Be}_{\text{I}})$ complex near nitrogen is markedly different from that in GaAs. In the +1 state it is like a Be-Be dimer on the Ga site, with both beryllium atoms at about the same distance from the ideal cation position. In the charge-neutral state, the Be dimer moves toward nitrogen and in the −1 state this defect should be considered as (Be-N) split-interstitial defect with the remaining beryllium quite close to the ideal Be_{Ga} position. The formation energies of Fig. 1 suggest the negative-U effect, which is also reflected in the strong geometric changes.

We checked three orientations of the (Be-N) dimer at the As (Ga) site: (1) along the (100) direction, (2) along (111) with beryllium between the nitrogen and the gallium (arsenic) atom, and (3) along (111) with nitrogen between the beryllium and the gallium (arsenic) atom. For the As site, only cases 1 [denoted $(\text{Be-N})_{\text{As(100)}}$ from here on] and 2 $[(\text{Be-N})_{\text{As(111)}}]$ are stable and case 3 relaxes into 1. $(\text{Be-N})_{\text{As(111)}}$ is about 350 meV lower in energy compared to $(\text{Be-N})_{\text{As(100)}}$. For the Ga site, only cases 1 $[(\text{Be-N})_{\text{Ga}}]$ and 3 are stable and 2 relaxes into 1. However, the case 3 has about 1 eV higher formation energy than the case 1 and therefore we do not consider it any further. Also notice that N_{config} is 3 and 4, for the (100) and (111) oriented split-interstitials, respectively.

For the split-interstitial defect formed by nitrogen and silicon, there appears a bonding state near the bottom of the gap and an antibonding states high in the gap.[12] Nitrogen would like to form split-interstitial defect complexes with group IV atoms such as silicon, but not with group VI atoms, because in this case the p-like antibonding defect orbital becomes occupied. On the other hand, in the case of group II atoms, also the bonding defect orbital should be empty when located on the anion site. If (Be-N) is located on the cation site, however, the surrounding anion dangling bonds give two more electrons for the defect, and the bonding orbital should be occupied. The occupation of the bonding and antibonding states is similar to the (Si-N) split interstitial on the anion site. Therefore, we would at least expect $(\text{Be-N})_{\text{Ga}}$ to have higher binding energy than $(\text{Be-N})_{\text{As}}$, even if the formation would be unfavored for other reasons.

For $(\text{Be-N})_{\text{As(100)}}$ there is an ionization level and a corresponding one-electron state close to the CBM. Characterizing this as a bonding state is slightly dubious since the Be-N bond length increases with increasing negative charge state (cf. Table I). At the same time, both the Be and the N move closer to the surrounding gallium atoms, and more so with nitrogen. There would seem to be a stronger bonding character with the surrounding gallium atoms than between the Be and N atoms. On the other hand, this state has somewhat more localization to the nitrogen atom, which due to higher electronegativity of nitrogen suggests bonding character. The other (Be-N) defects are found stable only at the neutral charge state. In order to find traces of the (Be-N) related states, the Be and N local density of states are shown in Fig. 2. The bonding and antibonding states of $(\text{Be-N})_{\text{As(100)}}$ can also be distinguished here at the energies of about −0.5 and 0.6 eV, respectively. In the case of $(\text{Be-N})_{\text{As(111)}}$ we also observe a state just below VBM (mostly Be localized), at the energy of −0.5 eV. No clear peak in the conduction band (CB) can be found, but some increase in beryllium localization. Finally, $(\text{Be-N})_{\text{Ga}}$ produces a strong nitrogen-localized peak below the VBM. Similarly to $(\text{Be-N})_{\text{As(111)}}$, small increase in beryllium localization and decrease in nitrogen localization in the CB can be found.

TABLE II. The LDA calculated band gaps of selected configurations (in the units of eV).

Configuration	GaAs	GaAsN
Pure	0.530	0.387
Be_{Ga}	0.531	0.438
$(Be\text{-}N)_{As(100)}$		0.602
$(Be\text{-}N)_{As(111)}$		0.559
$(Be\text{-}N)_{Ga}$		0.518

Another characteristic of (Be-N) defects is the diminution of the Ga 3*d*-N 2*s* interaction evidenced by the disappearance of the three-peak splitting around −15 eV in Fig. 2. Also, as nitrogen becomes part of a defect complex, it loses its alloying properties in GaAsN. Especially in the $(Be\text{-}N)_{Ga}$ case, we do not really have GaAsN substitutional alloy any more, but rather a nitrogen derived localized defect in GaAs. The band gaps of selected configurations are given in Table II. We find out that beryllium doping has no effect on the band gap in pure GaAs (except of course for the large carrier concentration generated band-gap decrease[34] due to the hole correlation effects). However, in GaAsN, even a substitutional Be_{Ga} defect seems to partly destroy the long-range interactions of the neighboring nitrogen. Then, in the case of (Be-N) defects, the band gaps are similar to GaAs or higher, reflecting the localized nature of these defects. The band-gap increase is probably mostly due to the very high defect concentration in our model, which may push the valence and conduction-band edges. Similar band-gap increase was found in Ref. 13, but should converge to GaAs value as the supercell size grows bigger. High band-gap values could also be caused, at least partly, by the strain in the sample.

It is surprising to notice that, with the beryllium defects studied here, nitrogen proximity is *always* favored in defect formation, even if the mechanism is different for different defects.

It is also useful to compare our results to the results of Be-doped GaN.[9,10] In GaN, the Be_I has formation energy clearly below that of the Be_{Ga} defect. As a result, *p*-type doping of GaN with beryllium does not work, as all of the Be_{Ga} acceptors are compensated by the Be_I donors. This is just the opposite to what happens in GaAs and GaAsN, as can be seen from the Be_I and Be_{Ga} defect formation energies. Most of these differences can be understood with a strong Be-N bond. The higher formation energy for Be_{Ga} in GaN compared to GaAs is due to stronger (or more rigid) Be-N and Ga-N bonds in GaN compared to Be-As and Ga-As bonds in GaAs, respectively. Moreover, in GaN interstitial Be is located in the middle of a tetrahedron formed by nitrogen atoms, giving low formation energy for Be_I and consequently a very high barrier for the diffusion through interstitial sites.

C. Discussion

Now we can summarize and compare calculated results with those from the experiments presented in Sec. I.

First, the charge-carrier concentration of Be-doped GaAs drops when nitrogen is introduced, which seriously limits the usability of Be-doping on applications. This may be caused by higher ionization energy of Be_{Ga} or compensation by other defects. Unlike suggested in Ref. 1, we do not find an increase in the Be_{Ga} ionization energy when adding nitrogen to GaAs, although we should emphasize that the expected shift is smaller than our error margins. It seems that there has to be a compensating agent present. Our calculation suggests that this could be caused by either Be_I double donors, whose concentration increases especially near the Be_{Ga}-N_{As} complexes, and the neutral (Be-N) defects. The former has the lowest formation energy, making it the most likely cause. Among (Be-N) defects, as GaAsN growth is usually arsenic rich,[35] the $(Be\text{-}N)_{Ga}$ case should be the dominating type with also rather low formation energy. The unintentional doping of (In)GaAsN samples is usually of *p* type, so it seems unlikely that this causes the compensation. Moreover, it is interesting to note that thermal annealing does not improve the carrier concentration in solid-source molecular-beam epitaxy (MBE) grown GaAsN.[1] This could be partly due to the strength of the Be-N bond in (Be-N) defects. However, a very good recovery is achieved in gas-source MBE grown InGaAsN, where hydrogen plays an important role.[1,2]

Second, the nitrogen concentration of the sample increases when Be is introduced into the growth. Effect is rather dramatic as 10^{19} cm^{-3} of beryllium increases nitrogen concentration by about 10^{20} cm^{-3} atoms. Increased sticking of nitrogen on to the surface was again related to the strong Be-N bond,[1,4] but no actual mechanism has been proposed. Such mechanism is also beyond these calculations (surface calculations are required), but this still suggests that (Be-N) defects could be present at somewhat significant concentration.

As shown in Sec. III B, large concentration of (Be-N) defects should increase the band gap. Unfortunately, to the best of our knowledge, there is no experimental results on this. Especially, it is difficult to distinguish between effects due to the changes in the (Be-N) concentration, hole correlation effects, and increased In-N coordination in the case of InGaAsN. When trying to find traces of the (Be-N) defects, instead of looking at the band gap, it might prove more fruitful to employ Raman spectroscopy for finding the respective local vibrational modes. Moreover, x-ray spectroscopic methods, such as the resonant inelastic x-ray scattering (RIXS), could be used to probe the local electronic structure of the defects directly.

Finally, we consider how the above-mentioned processes might affect diffusion. Formation of Be_{Ga} is slightly preferred near nitrogen. This creates a defect-complex site on which further beryllium can be clustered [e.g., $(Be_{Ga}\text{-}Be_I)$ configuration]. The Be interstitial diffusion barrier was not largely affected by the nitrogen, but the clustering effects should decrease the diffusion coefficient (also recall, how the strong Be-N bond eliminated Be_I diffusion in GaN). Additionally, this site would act as a center for enhancing the rates of several reactions, such as the Ga_I-Be_{Ga} kick out or formation of $(Be\text{-}N)_{Ga}$ from Be_{Ga} and split interstitials [(N-N) or (N-As)].[36,37] We also find alternative paths for the direct kick-out process: beryllium coming from the interstitial site

squeezes between the gallium and the nitrogen to form $(\text{Be-N})_{\text{As}(111)}$, and from here proceeds to kick out the gallium. Also, $(\text{Be-Ga-N})_{(\text{GaAs})}$ could be an intermediate step in the kick-out process as the gallium pops out from between the Be_{Ga} and N_{As}. As nitrogen presence lowers the Ga vacancy formation energy, it would also increase the diffusion mediated by the vacancies, but interstitial beryllium is eager to fill all the available gallium vacancies.

IV. CONCLUSIONS

We have performed an extensive study of beryllium defects in GaAs and GaAsN. Formation energies of substitutional, interstitial, and a few cluster-type defects were calculated. We have also presented additional data, which can hopefully serve as a reference for the future work, even if not analyzed thoroughly in this paper.

The most complicating factor is the small size of both the beryllium and the nitrogen atoms, resulting in defect clustering and complexes and several competing configurations: most importantly the $(\text{Be}_{\text{Ga}}\text{-Be}_{\text{I}})$ and (Be-N) split interstitials. We expect the former to be the dominating factor in the charge-carrier compensation in GaAsN. The latter might also play a role, depending on their concentration, which is governed by the surface kinetics during growth. Creation of the (Be-N) defects, and to a smaller extent also Be_{Ga} near a nitrogen atom, was also found to modify the alloying properties of nitrogen in GaAsN. Most notably, the nitrogen effect on the well-known reduction in the band gap in GaAsN alloy is eliminated through the formation of (Be-N) defects.

Concerning the diffusion, agile interstitial beryllium diffusion was observed, which would then easily fill the available gallium vacancies. The above-mentioned defect clustering probably leads to a decreased beryllium diffusion and the kick-out mechanism is likely to get more pronounced with the alternative paths related to the $(\text{Be-N})_{\text{As}(111)}$ and $\text{Be}_{\text{I}(\text{tGa})}$ defects.

ACKNOWLEDGMENTS

This work was supported by the Jenny and Antti Wihuri Foundation and Tekniikan edistämissäätiö (H.-P.K.) and the Academy of Finland (E.A.). We are thankful for the Centre for Scientific Computing (CSC) and Material Sciences National Grid Infrastructure (M-grid, Akaatti) for the computational resources.

*hannu.komsa@tut.fi
†tapio.rantala@tut.fi

[1] T. Liu, S. Chandril, A. J. Ptak, D. Korakakis, and T. H. Myers, J. Cryst. Growth **304**, 402 (2007).
[2] W. Li, M. Pessa, J. Toivonen, and H. Lipsanen, Phys. Rev. B **64**, 113308 (2001).
[3] A. Fleck, B. J. Robinson, and D. A. Thompson, Appl. Phys. Lett. **78**, 1694 (2001).
[4] S. Y. Xie, S. F. Yoon, S. Z. Wang, Z. Z. Sun, P. Chen, and S. J. Chua, J. Cryst. Growth **260**, 366 (2004).
[5] J. Pakarinen, C. S. Peng, V. Polojärvi, A. Tukiainen, V.-M. Korpijärvi, J. Puustinen, M. Pessa, P. Laukkanen, J. Likonen, and E. Arola, Appl. Phys. Lett. **93**, 052102 (2008).
[6] J. Marcon, M. Ihaddadene, and K. Ketata, J. Cryst. Growth **253**, 174 (2003).
[7] R. Mosca, P. Bussei, S. Franchi, P. Frigeri, E. Gombia, A. Carnera, and M. Peroni, J. Appl. Phys. **93**, 9709 (2003).
[8] C. Wang and Q.-M. Zhang, Phys. Rev. B **64**, 195204 (2001).
[9] C. G. Van de Walle, S. Limpijumnong, and J. Neugebauer, Phys. Rev. B **63**, 245205 (2001).
[10] C. D. Latham, R. M. Nieminen, C. J. Fall, R. Jones, S. Öberg, and P. R. Briddon, Phys. Rev. B **67**, 205206 (2003).
[11] K. M. Yu, W. Walukiewicz, J. Wu, D. E. Mars, D. R. Chamberlin, M. A. Scarpulla, O. D. Dubon, and J. F. Geisz, Nature Mater. **1**, 185 (2002).
[12] A. Janotti, P. Reunchan, S. Limpijumnong, and C. G. Van de Walle, Phys. Rev. Lett. **100**, 045505 (2008).
[13] J. Li, P. Carrier, S.-H. Wei, S.-S. Li, and J.-B. Xia, Phys. Rev. Lett. **96**, 035505 (2006).
[14] G. Baldassarri H. v. H., M. Bissiri, A. Polimeni, M. Capizzi, M. Fischer, M. Reinhardt, and A. Forchel, Appl. Phys. Lett. **78**, 3472 (2001).
[15] A. Janotti, S.-H. Wei, S. B. Zhang, S. Kurtz, and C. G. Van de Walle, Phys. Rev. B **67**, 161201(R) (2003).
[16] A. Janotti, S. B. Zhang, S.-H. Wei, and C. G. Van de Walle, Phys. Rev. Lett. **89**, 086403 (2002).
[17] A. Amore Bonapasta, F. Filippone, and P. Giannozzi, Phys. Rev. B **68**, 115202 (2003).
[18] M.-H. Du, S. Limpijumnong, and S. B. Zhang, Phys. Rev. B **72**, 073202 (2005).
[19] C. G. Van de Walle and J. Neugebauer, J. Appl. Phys. **95**, 3851 (2004).
[20] C. W. M. Castleton, A. Hoglund, and S. Mirbt, Phys. Rev. B **73**, 035215 (2006).
[21] P. Deák, T. Frauenheim, and A. Gali, Phys. Rev. B **75**, 153204 (2007).
[22] Freysoldt *et al.* (Ref. 38) have recently introduced an improved method to include finite-size corrections (cf. the term ΔV in our calculations) for *ab initio* charged-defect supercell calculations. However, we are not employing their scheme in our present study.
[23] G. Kresse and J. Hafner, Phys. Rev. B **47**, 558 (1993).
[24] G. Kresse and J. Furthmüller, Comput. Mater. Sci. **6**, 15 (1996).
[25] G. Kresse and J. Furthmüller, Phys. Rev. B **54**, 11169 (1996).
[26] *Lange's Handbook of Chemistry*, 14th ed., edited by J. A. Dean (McGraw-Hill, New York, 1992).
[27] Choosing the Ga as the origin, As and N are located at $(\frac{1}{4},\frac{1}{4},\frac{1}{4})$, the center of arsenic tetrahedron at $(\frac{2}{4},\frac{2}{4},\frac{2}{4})$, and the center of gallium tetrahedron at $(\frac{3}{4},\frac{3}{4},\frac{3}{4})$. The coordinates are in the units of lattice constant.
[28] S. B. Zhang and J. E. Northrup, Phys. Rev. Lett. **67**, 2339 (1991).
[29] M.-A. Malouin, F. El-Mellouhi, and N. Mousseau, Phys. Rev. B **76**, 045211 (2007).

[30] F. El-Mellouhi and N. Mousseau, Phys. Rev. B **71**, 125207 (2005).
[31] J. Gebauer, M. Lausmann, F. Redmann, R. Krause-Rehberg, H. S. Leipner, E. R. Weber, and P. Ebert, Phys. Rev. B **67**, 235207 (2003).
[32] F. D. Auret, S. A. Goodman, and G. Myburg, J. Electron. Mater. **21**, 1127 (1992).
[33] Y. C. Pao, J. Franklin, and J. S. Harris, Jr., J. Cryst. Growth **95**, 301 (1989).
[34] M. Ilegems, J. Appl. Phys. **48**, 1278 (1977).
[35] F. Ishikawa, E. Luna, A. Trampert, and K. H. Ploog, Appl. Phys. Lett. **89**, 181910 (2006).
[36] S. B. Zhang and S.-H. Wei, Phys. Rev. Lett. **86**, 1789 (2001).
[37] K. Laaksonen, H.-P. Komsa, T. T. Rantala, and R. Nieminen, J. Phys.: Condens. Matter **20**, 235231 (2008).
[38] C. Freysoldt, J. Neugebauer, and C. G. Van de Walle, Phys. Rev. Lett. **102**, 016402 (2009).